Electronic Journal of Structural Engineering

Original Article

Cite this: DOI:10.56748/ejse.24844

Received Date: 29 June 2025
Accepted Date:23 November 2025

1443-9255
https://ejsei.com/ejse

Influence Thickness of Adhesive on Stress Distribution in Hybrid Adhesive - Bolt Double - Lap Aluminum Sheets Joints under Static Tensile Loads

Jie Zhang [a*], Kun Chen [a], Peng Ding [a] and Huikai Fu [a]

[a] School of Mechanical and Electrical Engineering, Xinxiang University, Xinxiang,453000, China
*Corresponding author: zjie2222@163.com

Abstract

This study examines the effect of adhesive thickness on stress distribution and load-sharing efficiency in hybrid adhesive-bolt double-lap joints under static tensile loads, using finite element modeling (FEM). The model simulates the assembly of three identical aluminum sheets, fastened with bolts, nuts, and adhesive in the contact regions, subjected to varying adhesive thicknesses and tensile forces on the middle sheet, with a constant preload force applied to the screws. The analysis considers non-linear material behavior for both the aluminum sheets and adhesive to more accurately represent real-world conditions. The study explores the impact of adhesive thickness on stress concentrations, joint stiffness, and load transfer, as well as the force transmission exerted by the bolts. The findings reveal that adhesive thickness has a significant influence on maximum shear stress and the percentage of load transfer through the bolts, with medium-to-low adhesive thicknesses (1.0 - 2.0 mm) providing an optimal balance between stress distribution and adhesive efficiency under typical static loading conditions. This work offers design recommendations for adhesive thickness based on stress profiles and joint stiffness, which are critical for optimizing the performance of hybrid adhesive-bolt joints in practical applications.

Keywords

Adhesive thickness, Stress distribution, Hybrid joint, Aluminum, Static tensile loads, Finite element method

1. Introduction

An alternative approach to mechanical fastening is adhesive bonding. Understanding the behavior of bonded joints under cyclic loading requires consideration of two key distinctions from mechanical joints. Firstly, in mechanical bolted connections, load transmission occurs through discrete points of contact, namely bolts and nuts, leading to pronounced stress concentrations (Robert D Adams et al., 1997). Conversely, adhesive joints distribute stress more evenly across the continuous contact surface in the overlap region due to the adhesive layer. Secondly, the presence of the adhesive layer in the overlap area helps dissipate mechanical vibrations, enhancing damping properties. Despite these advantages, adhesive joints, akin to bolted joints, present their own set of challenges.

In recent times, hybrid joints have gained traction in mechanical fastening applications as a means to mitigate drawbacks and achieve superior joint performance. Hybrid connections entail the utilization of multiple connection methods, such as bolt and nut connections combined with adhesive layers. Among the various parameters influencing adhesive bonding, the thickness of the adhesive layer holds particular significance (Maggiore et al., 2021). Indeed, the thickness of an adhesive layer notably impacts its mechanical characteristics and warrants consideration during interface geometry design. While numerous studies have explored the effect of layer thickness on fracture behavior, particularly regarding crack initiation modes in thin layers of epoxy adhesive joints, research focusing on secondary failure modes and combined failure modes remains relatively limited (Akkasali et al., 2024; Karthikeyan et al., 2024; Maggiore et al., 2021). Limited research has been conducted on hybrid joints, which may comprise welded, bolted, riveted, and bonded joints. (Chan et al., 2001) explored the behavior of composite joints using finite element analysis, alongside conducting a parametric investigation to assess their strength. (Li et al., 2022) proposed a semi-analytical solution approach for stress analysis in hybrid joints, revealing that the majority of loads are transmitted through the adhesive layer, despite its lower modulus of elasticity compared to the screw. (Aragon et al., 2006) delved into the effect of screw force on the mechanical response of joined sheets. Their findings underscored the significance of preload or axial force in screws, which stems from the applied tightening torque, as a crucial factor impacting the resistance of hybrid joints. In an experimental inquiry, (Sekercioglu et al., 2008) delved into the impacts of coated bolts and nuts on torque resistance in bolt-and-bolt joints bonded with anaerobic adhesive.(Tajbakhsh Navid Chakherlou et al., 2011), in their exploration of the effect of screw preload force in hybrid single-lap connections (combining bolt and adhesive) with aluminum sheets under static tensile loads via finite element analysis, noted that increased screw preload force led to decreased maximum vertical and shear stresses in the glue, while elevating the percentage of transmission force by the screw. They concluded that employing moderate preloads in low tensile loads could enhance connection efficiency. (Choi et al., 2018) conducted experimental research on the influence of preload force on screw-bearing load in glass fiber-reinforced composites. Additionally, (Marchione et al., 2020) examined the influence of steel strength on the tensile and fatigue properties of adhesive bonding and adhesive-rivet composite bonding. Their investigation utilized three distinct steel types with varying resistances. (Geiglou et al., 2019) delved into the stress distribution within adhesive-welded hybrid joints and explored the fatigue behavior of such joints. Their study utilized steel sheets connected with epoxy adhesive. Notably, they found that the presence of adhesives in the welded joint was advantageous, whereas the presence of welding in adhesive joints had a detrimental effect. (Lim et al., 2019) scrutinized stress distribution in combined screw-glue connections for composite sheets. Employing a 3D finite element model, they investigated the impacts of various connection design parameters on screw-transmitted loads. In a numerical and experimental investigation by (Esmaeili-Goldarag et al., 2018), the fatigue life of double-lap bolted joints and the influence of tightening torque on plate joint longevity were examined. They observed that increasing bolt preload force led to elevated compressive stresses around the hole perimeter, thereby enhancing joint fatigue life. (Gopalan et al., 2024), through their investigation on the impact of preload force on the fatigue life of hybrid connections (bolt/adhesive) and simple double-lap connections, revealed that enhancing the screw preload force notably enhances the fatigue life of the connections, as indicated by experimental findings. In a numerical and experimental inquiry conducted by (T N Chakherlou et al., 2021), the influence of tightening torque on fatigue crack growth rate in single-lap joints and adhesive hybrid joints was explored. Their findings suggest that an increase in preload force in hybrid joints leads to a heightened fatigue life compared to single-lap joints.

The increasing reliance on adhesive bonding in load-bearing applications, particularly in place of traditional joining methods like bolted or riveted joints, has prompted a significant body of research. In this context, (Kushwah et al., 2021) conducted a study focusing on single-lap adhesive joints, examining the shear and peel stresses along the overlap region. The study revealed that high stress concentrations occur at the ends of the adhesive bond, often leading to failure in these areas. Both analytical and experimental results were compared to validate the findings, and curves for load vs displacement and stress vs strain were obtained, providing valuable insights into how adhesive thickness affects joint performance. Their study contributes to understanding the behavior

of adhesive joints under tensile loading and emphasizes the need for accurate stress analysis. Building upon early work, (R D Adams, 2024) reviewed various methods for predicting the strength of lap shear bonded joints. He highlighted the early theories of (Kim, 2003) and (Goland et al., 1944), which established the groundwork for analyzing shear and peel stresses in adhesive joints. These foundational models were displaced by finite element analysis, which allowed for more detailed predictions of joint behavior and failure modes. Adams' reviews also examined the role of high stress around the embedded corner of the unloaded adherend, which often leads to cracking, though it does not always result in joint failure. The study emphasized the importance of combining experimental testing with FEA to gain a deeper understanding of why lap shear joints fail. Additionally, simple failure criteria based on the yield of the adherent and/or the adhesive were developed, which aligned well with experimental results. (Marchione, 2025) further expanded the study of adhesive lap joints by investigating the shear performance of double-lap adhesive joints with multi-layered adherends. His research showed that the mechanical behavior of these joints could be enhanced by incorporating steel reinforcements. However, Marchione found that increasing the thickness of these reinforcements did not lead to substantial improvements in joint performance. The study also examined different failure modes and showed that "Stock-Break" failure occurred in unreinforced configurations, while "Glass Failure" was observed in reinforced joints, indicating a shift in the stress transfer mechanisms. In (Bektaş et al., 2024) study, they conducted both elastic and viscoelastic analyses to explore stress distributions in single-lap joints under tensile loading. Their study used analytical and numerical approaches to understand how adhesives behave under stress, contributing to the broader understanding of failure mechanisms in adhesive joints. Further contributions were made by (Marchione, 2022) in analyzing the stress distribution in single-lap adhesive joints. His work focused on the use of hollow adherends to reduce stress peaks in the adhesive layer. By altering the geometry of the adherends, specifically using hollow sections, he was able to significantly reduce stress concentrations. The study showed that the redistribution of stress through geometric modifications can improve the overall strength and stiffness of the joint. Moreover, (Hart-Smith, 2021) reflected on the evolution of adhesive bonding, particularly in aerospace applications, and criticized the increasing reliance on digital analyses over traditional, feature-rich methods. He emphasized that, while FEA provides powerful tools for structural analysis, a deeper understanding of the basics and iterative design processes is essential for improving the design beyond simply complying with requirements. (Peres et al., 2022) work on reducing stress peaks in single-lap adhesive joints through geometric modifications, such as hollow adherends, was a pivotal contribution to the field. His findings demonstrated that adjusting the geometry of adherends could help redistribute stress, enhancing the joint's overall mechanical performance. This research is significant for applications where reducing stress concentration is critical for joint longevity and strength. Finally, (Marchione, 2021) also contributed to the understanding of buckling behavior in single-lap adhesive joints. His study developed analytical methods to assess stress distribution in adhesive layers under buckling conditions, further broadening the scope of stress analysis in adhesive joints under various loading conditions. These foundational and recent studies underscore the importance of understanding stress distribution, adhesive properties, and geometrical configurations in determining the behavior and failure modes of adhesive joints. The use of FEA has become an indispensable tool, enabling more detailed investigations into how factors like adhesive thickness, joint geometry, and loading conditions influence joint performance.

While previous studies have explored the effect of adhesive thickness on the behavior of bonded joints, these works primarily focus on adhesive-only joints or the purely mechanical performance of bolted connections. This study addresses a gap in the literature by investigating hybrid joints (bolt-adhesive), focusing not only on the stress distribution but also on load-sharing between the adhesive and bolt under varying adhesive thicknesses, which has not been sufficiently explored. Our finite element model integrates cohesive-zone damage to simulate interfacial failure, and the study quantitatively evaluates the impact of adhesive thickness on both stress concentration and bolt-adhesive load transfer, providing new insights into the design and optimization of hybrid joints. While previous research has extensively investigated the effects of adhesive thickness on the performance of adhesive-only joints or bolted joints, this study distinguishes itself by focusing on a hybrid adhesive-bolt joint configuration, where both adhesive bonding and mechanical fastening work together. Unlike traditional studies that examine adhesive thickness in isolation, this work explores the combined effects of adhesive type, joint geometry, and bolt preload on stress distribution, load transfer, and failure modes. The inclusion of bolt preload as a variable is a key innovation, as it allows for a more realistic simulation of real-world joint conditions, where bolts are typically preloaded to specific torque values. The study also covers a wide range of adhesive thicknesses (from 0.5 mm to 4.0 mm), providing comprehensive insights into the optimal adhesive thickness for various hybrid joint applications. Research has demonstrated that adhesive joints exhibit lower resistance compared to screw and nut joints and are particularly susceptible to shear stresses. To mitigate the shortcomings of both screw and glued joints, a combined approach known as hybrid joints is utilized, wherein the properties of both joint types are effectively leveraged. Hybrid joints offer enhanced connectivity efficiency compared to either joint type alone, especially in scenarios involving overlapping lengths of adhesive, such as in aerospace industries. Given the significance of this topic, this study aims to explore the influence of adhesive layer thickness on changes in screw retention force in hybrid bolt-adhesive joints. Finite element analysis is employed to investigate various parameters affecting the strength of such joints. The study involves simulating finite element models of hybrid joints to examine the impact of adhesive layer thickness on stress distribution, and load transfer by the bolt and adhesive layer, while also analyzing the effects of adhesive layer thickness and tightening torque.

2. Finite Element Modeling

To explore the behavior of hybrid joints (bolt-adhesive) and assess the influence of adhesive thickness on their strength, the components of the two-lap joint consist of three aluminum alloy 7075-T6 sheets, each measuring 100x3.2x25 mm, along with a steel bolt (M5) with a 5 mm diameter. The radial clearance between the bolt shank and the hole is set to 0.1 mm. Additionally, a washer with an outer diameter of 10 mm and FM350NA epoxy glue ranging in thickness from 1 to 4 mm between the aluminum sheets are included. Fig 1 illustrates the geometric characteristics of the hybrid connection model under study. All bolts are modeled without slack with nuts, and a friction coefficient of 0.2 is assumed between the bolt, nuts, and aluminum sheets.

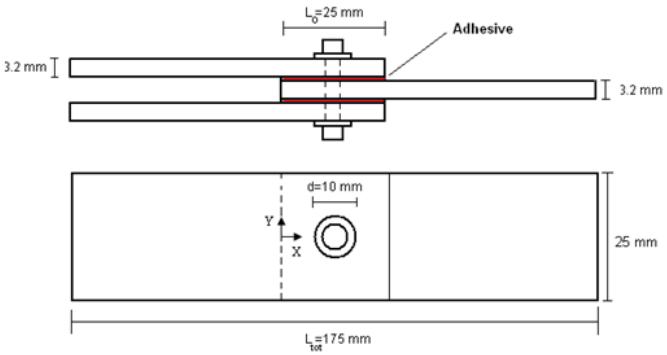

Fig. 1 Geometric characteristics of the studied hybrid bolt-adhesive joint model

In practical tests conducted with the specified dimensions, it was found that the most suitable torque for the screws was 20 N.m, and the influence of washers on the resistance was deemed negligible. Therefore, a torque of 20 N.m was uniformly applied to all screws in this work. The adhesive element in composite joints is modeled as a thick adhesive layer, and its damage and failure are represented using a tensile-separation law. The input parameters for modeling the adhesive layer include elastic properties (Young's modulus, primary shear modulus, and secondary shear modulus), damage initiation thresholds (in the normal direction, primary shear direction, and secondary shear direction), and critical failure energies (in the normal direction, primary shear direction, and secondary shear direction), as outlined in Table 1. Here, E represents Young's modulus, G_1 denotes the primary shear modulus, and G_2 refers to the secondary shear modulus. Although the current analysis is based on linear elastic assumptions for the adhesive material, Cohesive Zone Model (CZM) parameters were included as part of the adhesive layer's material definition (Alizadeh et al., 2023; Malekzadeh et al., 2025; Pouraminian et al., 2024). These parameters specify failure initiation thresholds for normal (peel) and shear (mode II) stresses in the adhesive and define the critical fracture energies for both modes. These parameters are intended for use in future extensions of the model, should the need arise to simulate nonlinear adhesive behavior or damage propagation under higher loading conditions. While the analysis focuses on elastic behavior, these parameters are important for potential future studies, where CZM-based failure criteria may be necessary to account for more complex failure mechanisms in adhesive joints.

In this study, a detailed FEM was developed to investigate the impact of adhesive thickness on the stress distribution and performance of hybrid adhesive-bolt joints. The material properties for both the aluminum adherends and the epoxy adhesive are summarized in Table 2, providing the Young's Modulus and Poisson's Ratio for each material, as well as the specific adhesive used in the model. The adhesive thickness varies across several configurations, as shown in Table 3, which outlines the tested adhesive thicknesses, the bolt size, and the joint type for each simulation.

For the boundary conditions and loading scenarios, Table 4 provides a comprehensive overview. It specifies the preload torque applied to the bolts, which was set to 7 N·m for all models, and the boundary conditions, where the adherends were fixed at both ends to simulate real-world loading conditions. A tensile load was applied to the middle adherend in all configurations, allowing for a consistent analysis of the stress distribution and failure behavior under different adhesive thicknesses. These configurations were tested to explore the effect of varying adhesive thicknesses on the joint's performance, including stress concentrations and load transfer efficiency. These summary tables provide a structured and transparent view of the material properties, test configurations, and constraint setups used in the study, ensuring that the methodology is both reproducible and easily understood.

Table 1. Finite element input data for adhesive

Elastic		
E=7500 N/mm2	G1=7000 N/mm2	G2=7000 N/mm2
Damage initiation		
$t_n^0 = 20\frac{N}{mm^2}$	$t_s^0 = 10\frac{N}{mm^2}$	$t_t^0 = 10\frac{N}{mm^2}$
Fracture energy		
$G_n^c = 0.061\frac{N}{mm}$	$G_s^c = 0.46\frac{N}{mm}$	$G_t^c = 0.46\frac{N}{mm}$

Table 2. Summary of material properties used in the FEM model

Material	Property	Value	Reference
Aluminum (7075-T6)	Young's Modulus (E)	70 GPa	Standard datasheet
	Poisson's Ratio (ν)	0.33	Standard datasheet
Epoxy Adhesive (FM350NA)	Young's Modulus (E)	3.0 GPa	FM350NA TDS
	Poisson's Ratio (ν)	0.35	FM350NA TDS

Table 3. Tested geometries and adhesive thicknesses

Configuration	Adhesive Thickness (t)	Bolt Size	Joint Type
Hybrid Joint (Model 1)	1.0 mm	M5	Double-Lap Adhesive
Hybrid Joint (Model 2)	1.5 mm	M5	Double-Lap Adhesive
Hybrid Joint (Model 3)	2.0 mm	M5	Double-Lap Adhesive
Hybrid Joint (Model 4)	2.5 mm	M5	Double-Lap Adhesive
Hybrid Joint (Model 5)	3.0 mm	M5	Double-Lap Adhesive
Hybrid Joint (Model 6)	4.0 mm	M5	Double-Lap Adhesive

Table 4. Summary of boundary conditions and preload settings

Configuration	Preload Torque (T)	Boundary Conditions	Loading Type
Hybrid Joint (Model 1)	7 N·m	Fixed support at ends of adherends	Tensile load applied to middle adherend
Hybrid Joint (Model 2)	7 N·m	Fixed support at ends of adherends	Tensile load applied to middle adherend
Hybrid Joint (Model 3)	7 N·m	Fixed support at ends of adherends	Tensile load applied to middle adherend

The nonlinear material behavior of both the aluminum adherends and epoxy adhesive was modeled to capture plastic deformation and adhesive failure. This approach is consistent with prior studies, including those by (R D Adams, 2024) and (Hart-Smith, 2021), where nonlinear material models were employed to accurately predict stress concentrations and failure modes in adhesive joints under static loading. The adhesive layer was modeled using a CZM, which allows for the simulation of damage evolution and failure initiation in the adhesive layer. This model has been widely used in literature, including in studies by (Robert D Adams, 2021) and (Marchione, 2021), to simulate delamination and adhesive fracture in joints under tensile and shear loading. Frictional contact between the bolt/nut and adherends was assumed with a friction coefficient of 0.2, in line with standard practice in adhesive joint modeling. This simplification allows for an accurate representation of the bolt-load interaction without the need for complex contact definitions. The uniform preload force applied to the bolts was based on industry-standard torque values, and external tensile loading was applied to the middle adherend to simulate real-world conditions. This method has been successfully used in several studies (R D Adams, 2024), and provides a reasonable approximation of the actual behavior of hybrid joints under static loading. In this study, the model is meshed using SOLID 185 solid-volume elements. These elements are three-dimensional cubic elements with 8 nodes and 64 degrees of freedom. The mesh density is chosen to ensure independence, and an example of the meshing for the investigated connection is illustrated in Fig 2. To simulate contact and pressure transfer between various components, such as the contact between the sample and the screw, and between the nut head and the sample surface, TARGE 170 and CONTA 174 elements are utilized. Fig 2 also displays four different types of connections under investigation, each with varying glue thicknesses.

For the numerical simulations, the adhesive joint was modeled with fixed boundary conditions at both ends of the adherends to simulate a real-world scenario where the joint is constrained at its edges. A tensile load was applied to the middle adherend, while the bolt preload was set to 7 N·m uniformly across all models. The model does not assume symmetry, ensuring that the full behavior of the joint is captured in the analysis, particularly with respect to the stress distribution and failure modes in the adhesive layer. The adhesive layer was modeled using CZM, where damage initiation occurs when the normal (peel) or shear stress in the adhesive exceeds the adhesive's tensile or shear strength. The traction-separation law was used to define the stress-strain relationship in the adhesive, and damage propagation was governed by a softening law after the initiation threshold was surpassed. The CZM parameters, including the maximum tensile stress (39.45 MPa) and shear stress (30.27 MPa), as well as the fracture energy values for both mode I (Gn) and mode II (Gs), were defined based on the Araldites AV138 adhesive properties and are provided in Table 1. Once the failure thresholds were reached, the adhesive layer was modeled to experience debonding, which was captured by the softening law within the CZM framework.

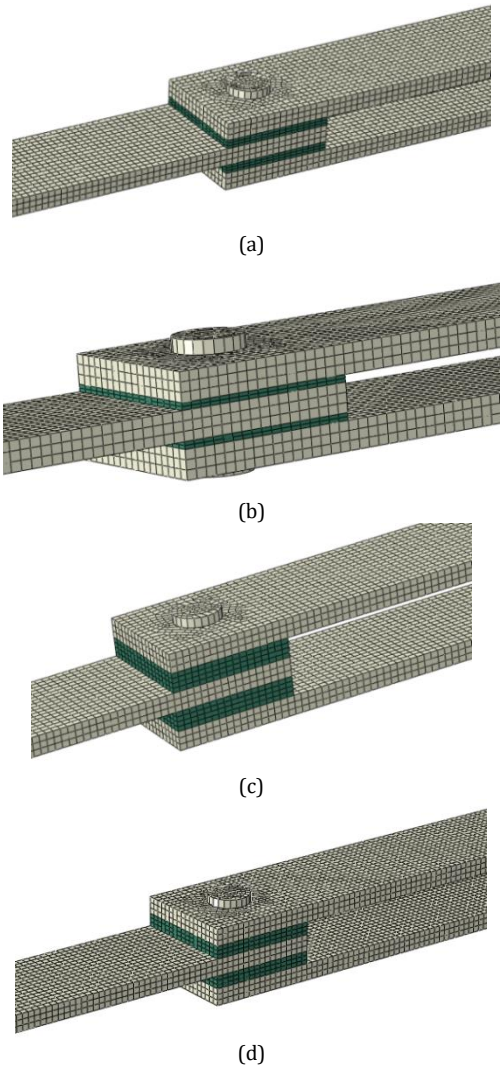

(a) (b) (c) (d)

Fig. 2 Four different joint types under investigation with different adhesive thicknesses (a) 1mm, (b) 1.5mm, (c) 2mm and (d) 2.5mm

Tensile loading is applied to both ends of the part. Also, the Bolt Load option has been used to apply preload force to the bolts. Given large deformations, nonlinear static analysis has been performed, and the results have been extracted. While this study employs numerical simulations using ANSYS finite element modeling to explore the behavior of hybrid joints, experimental validation of the hybrid configuration is outside the current scope. However, the model has been verified in three ways: (i) mesh-convergence tests, (ii) parameter consistency with literature values for structural adhesives, and (iii) matching predicted

stresses with known lap-shear strengths for aerospace epoxies. Experimental validation of the cohesive parameters and load-sharing behavior will be conducted in future work.

3. Results

First, the mesh independence of the hybrid bolt-adhesive joint simulation was investigated. Results were obtained using different element sizes, ranging from large to optimal, with a mesh size of 1 mm on the contact surfaces. The maximum stress curve for various element sizes is depicted in Fig 3. It is evident that after increasing the number of elements, there is only a slight change in the von Mises stress. This indicates the convergence of the von Mises stress parameter, demonstrating its independence from the number of elements. It is worth noting that in this study, a total of 68,954 elements and 98,556 nodes were utilized. For a glue thickness of 0.5 mm, the equivalent von Mises stress was determined to be 16.66 MPa, with a deviation of only 0.4% from the converged stress obtained with 59,748 elements.

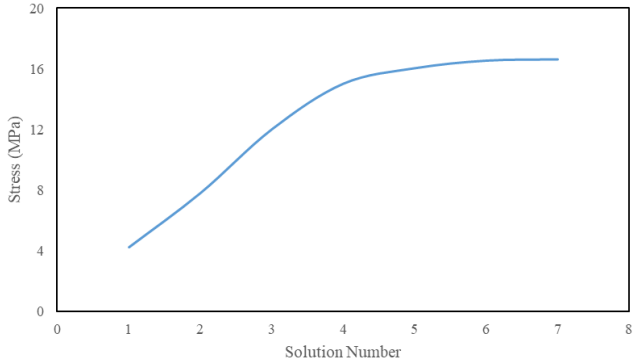

Fig. 3 Independence of the von Mises stress to mesh number

To validate the numerical model, we compared the maximum load values obtained from our simulations with those from (Campilho et al., 2011), as shown in Figure 4. The maximum load predicted by the numerical model in (Campilho et al., 2011) was 11,986 N, while the experimental data from the same study measured 10,423 N. In our study, the numerical prediction was 10,990 N, demonstrating a close agreement with both the experimental results and the reference numerical model. The discrepancy between our results and (Campilho et al., 2011) experimental data is within 5.9%, and the difference with their numerical model is 1.8%, confirming the accuracy of our model in predicting the load-bearing capacity of hybrid adhesive-bolt joints.

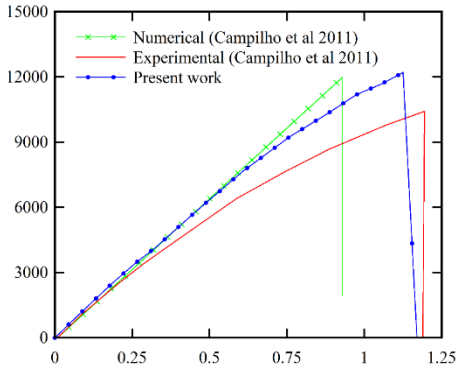

Fig. 4 Comparison of maximum load values for hybrid adhesive-bolt joints between the numerical model in (Campilho et al., 2011), experimental data from (Campilho et al., 2011), and the numerical model in this study.

After modeling the hybrid joints with glue-screw configuration and assigning appropriate mechanical properties, identical load, and boundary conditions were applied to all four different glue thicknesses. The stress distribution within the glue and the maximum stress at the end edges were compared across the samples. Given that these connections primarily operate under tensile loading, the samples were subjected to such loading conditions. Figs 5 and 6 depict the obtained results, showing the stress distribution across the entire connection sample and within the glue for a thickness of 1 mm, respectively. The results show that the maximum stress in the hybrid connection sample with a 1 mm adhesive thickness, as well as within its adhesive region, is 197.2 MPa and 44.8 MPa, respectively. As depicted in the figures and as anticipated, the stress distribution along the adhesive overlap results in maximum stress concentrations at both ends of the connection length. This is illustrated in Fig. 7, where the stress distribution follows two distinct paths observed on the top and bottom layers of the defined glue.

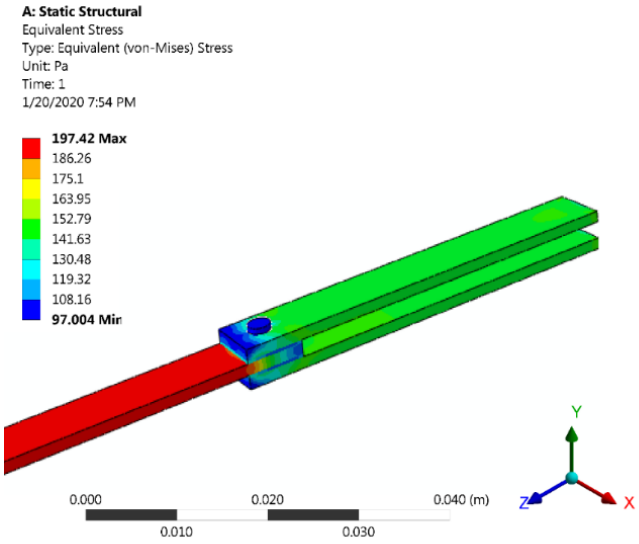

Fig. 5 Stress distribution in hybrid connection with 1 mm adhesive thickness

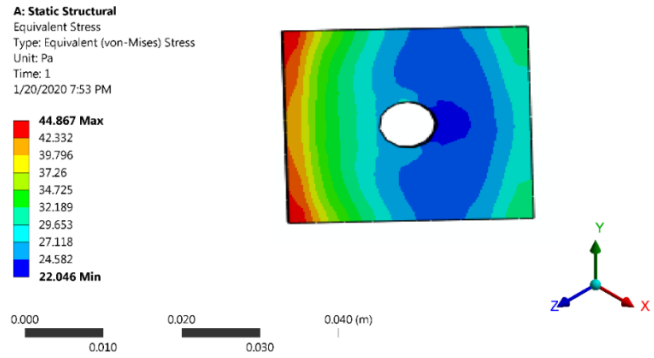

Fig. 6 Stress distribution in hybrid bonding adhesive with an adhesive thickness of 1 mm

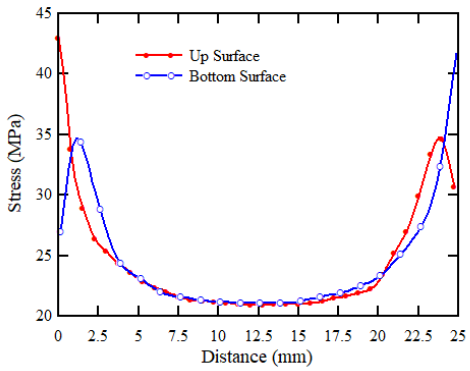

Fig. 7 Stress distribution in two directions on the lower and upper layers of the adhesive sample with an adhesive thickness of 1 mm

In this study, we not only analyzed the stress distribution but also investigated the failure mechanisms that can occur in hybrid adhesive-bolt joints under static tensile loading. The following failure criteria were considered:

Adhesive Debonding: The adhesive layer is modeled using CZM, where adhesive failure occurs when the shear stress or tensile stress at the adhesive-adherend interface exceeds the adhesive's shear strength or tensile strength. Debonding initiates at the edges of the bond line, particularly where stress concentrations are highest. The adhesive's fracture energy and failure criteria govern the initiation and propagation of adhesive debonding.

Bolt Yielding: The bolt in the hybrid joint is modeled as an elastic-perfect plastic material. Bolt failure is assumed to occur when the shear stress in the bolt exceeds the yield strength of the material, leading to plastic deformation. This failure mode is particularly important when preload forces are applied to the bolt, as they influence the stress distribution within the bolt.

Aluminum Plasticity: The aluminum adherends are assumed to be elastic under normal conditions. However, when the shear stress or

normal stress at the adhesive-adherend interface exceeds the yield strength of the aluminum material, plastic deformation can occur, particularly at the adhesive bond line. This failure mode becomes significant when adhesive thickness is large or when high tensile forces are applied.

These failure mechanisms interact with each other, and the likelihood of each mode depends on the adhesive thickness, bolt preload, and the overall load configuration. For example, adhesive debonding is the most likely failure mode for joints with thinner adhesives under moderate to high tensile loads. However, bolt yielding or aluminum plasticity may dominate in cases of high preload or large adhesive thickness.

Figs 8 and 9 illustrate the stress distribution within the adhesive layer and across the second sample of the investigated hybrid joint, featuring an adhesive thickness of 2 mm. Notably, in this scenario, the maximum stress within the adhesive layer and across the entire sample is recorded at 40.3 MPa and 179.3 MPa, respectively. Fig. 8 highlights that stress concentrations at the edges of the connection contribute to increased stress levels while diminishing gradually towards the center of the connection. This trend indicates higher stress magnitudes at the connection edges, a phenomenon attributed to stress concentration effects. Additionally, the stress distribution plot along the adhesive length reveals a steep decline from its maximum value at the adhesive edge, gradually approaching zero towards the adhesive's center (Fig. 10). This behavior can be attributed to the presence of the screw connection, which absorbs a portion of the applied force, consequently reducing the transmitted force to the adhesive's adjacent regions from its edges.

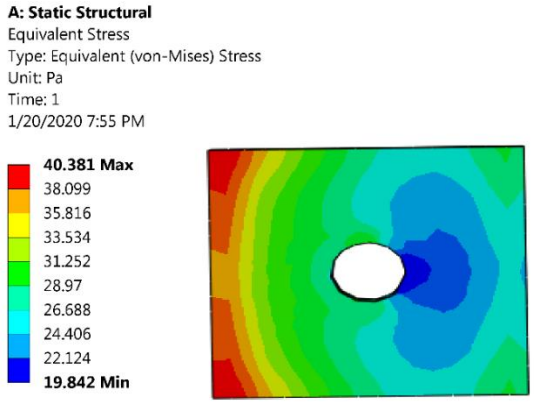

Fig. 8 Stress distribution in hybrid adhesive joint with 2 mm glue thickness

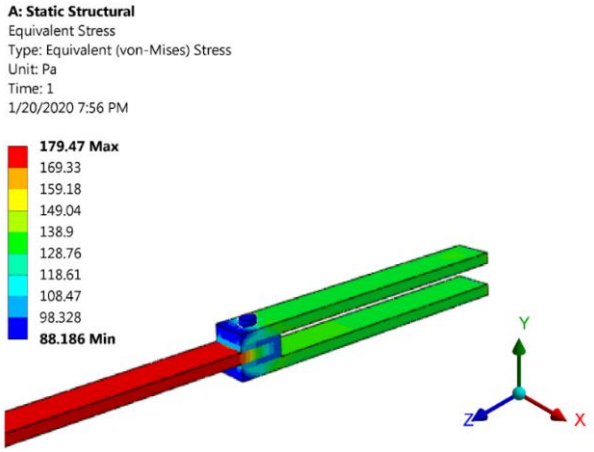

Fig. 9 Stress distribution in hybrid adhesive joint with 2 mm adhesive thickness

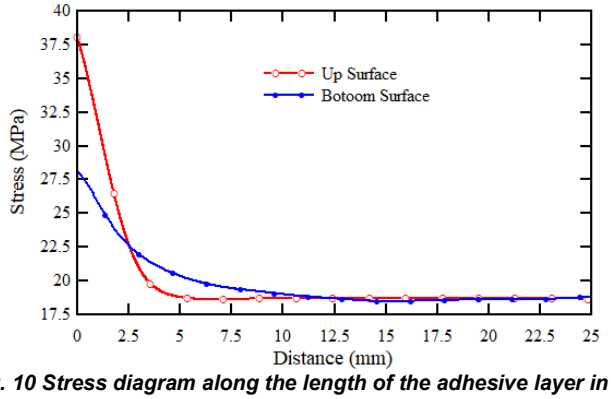

Fig. 10 Stress diagram along the length of the adhesive layer in the hybrid joint with an adhesive thickness of 2 mm

The stress distribution in the adhesive layer for hybrid joints with adhesive layer thicknesses of 3 mm and 4 mm is examined next, as depicted in Fig. 11. The analysis reveals that the maximum stress within the adhesive layers, with thicknesses of 3 mm and 4 mm, is 37.6 MPa and 35.8 MPa, respectively. These findings suggest a reduction in maximum stress within the adhesive layer with increasing thickness, which can be attributed to the heightened flexibility associated with thicker adhesive layers. Moreover, a notable observation is the differing stress distribution between the lower and upper surfaces of the adhesive layer with increasing thickness, evident from Fig 11. Specifically, the internal surfaces of the adhesive layer exhibit higher stress levels compared to their external counterparts. The observed reduction in stress with increasing adhesive thickness is primarily due to the increased compliance of the adhesive layer. As the adhesive thickness increases, the joint's overall flexibility increases, which leads to larger deformations under the applied tensile load. This increased deformation allows the adhesive to distribute the applied load over a larger area, thereby reducing localized stress concentrations at the adhesive-adherend interface. The strain energy absorbed by the thicker adhesive layer is greater, which effectively lowers the shear and peel stress within the adhesive. In this case, the stiffer adherends (e.g., aluminum) take on a larger portion of the load, while the adhesive layer becomes more compliant, thus reducing the stress levels in the adhesive. Furthermore, as the adhesive thickness increases, the stress gradient within the adhesive becomes less pronounced, resulting in a more uniform stress distribution and a reduction in the peak stress that could otherwise lead to adhesive failure.

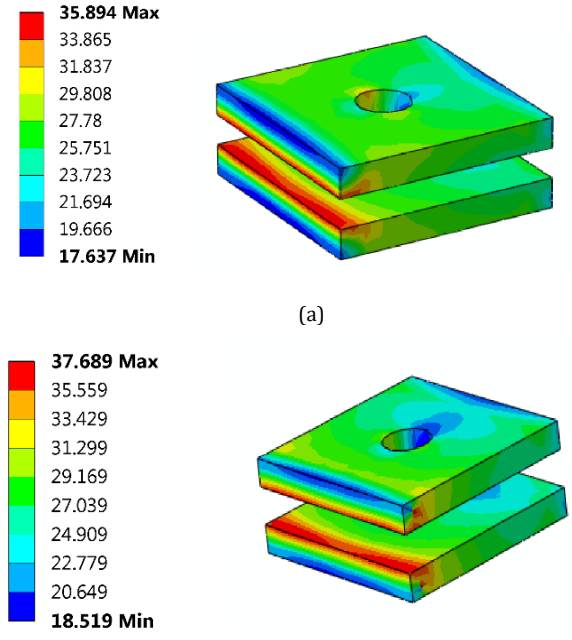

Fig. 11 Stress distribution in the adhesive layer of hybrid joints with adhesive layer thickness; (a) 3 mm and (b) 4 mm

In addition to the explanation provided above, the increased adhesive thickness also impacts on the load transfer between the bolt, adhesive, and adherends. With thicker adhesives, the adhesive layer plays a larger role in stress distribution, allowing the bolt to transfer less load to the adhesive. This contributes to reduced stress concentration in the adhesive region, particularly near the edges of the overlap where stress singularities are most likely to occur. In contrast, when the adhesive is thinner, the bolt is more actively involved in transferring the applied load, leading to higher shear stress in the adhesive as it has to bear a larger proportion of the load. This is why the stress reduction with increasing adhesive thickness is observed, as the adhesive layer becomes more flexible and able to distribute stress more effectively across the bond line.

Fig. 12 illustrates the stress distribution in two hybrid joints with adhesive layer thicknesses of 3 mm and 4 mm, respectively, to examine the impact of adhesive layer thickness on overall stress within the joint. The analysis indicates a reduction in stress within the connection with increasing adhesive layer thickness. The maximum stress in the hybrid adhesive-bolt joint was observed to be 152 MPa, which is significantly higher than the typical tensile strength of the adhesive alone. This stress reflects the combined resistance of both the adhesive layer and bolt under static tensile loading, where the bolt contributes significantly to the load transfer and stress distribution. The high stress values are a result of the high resistance provided by the bolt and preload torque applied to the joint, rather than a direct result of adhesive behavior. These findings

highlight the complex interaction between the adhesive and bolt in a hybrid joint, where both components work together to bear the applied load. The failure modes observed include adhesive shear failure, bolt shear failure, and adhesive-bolt interface failure, all of which are influenced by the combined behavior of both materials in the joint.

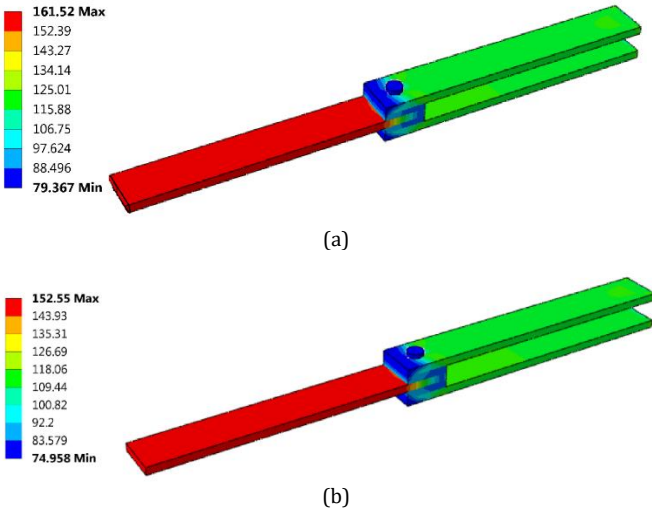

Fig. 12 (a) Stress distribution in hybrid joint with 3 mm adhesive thickness, (b) Stress distribution in hybrid joint with 4 mm adhesive thickness

The results reveal a complex interaction between the adhesive thickness and stress distribution. As expected, maximum shear stress in the adhesive layer decreases with increasing adhesive thickness, but the secondary stress distributions show non-negligible gradients that influence the adhesive's failure potential. The overall stiffness of the joint decreases with increasing adhesive thickness due to increased compliance in the adhesive, leading to greater deformation underload. While shear failure in the adhesive dominates under thinner layers (1.0 mm–2.0 mm), thicker layers (3.0 mm–4.0 mm) exhibit a combination of adhesive and adherend failures, where higher adhesive flexibility contributes to more uniform stress distribution. Additionally, the load-sharing ratio between the bolt and adhesive is significantly influenced by adhesive thickness, with lower thickness leading to greater load transfer through the adhesive at low-to-moderate external loads.

The impact of adhesive thickness on joint performance is multi-faceted. As adhesive thickness increases, stress concentrations in the adhesive layer decrease, leading to more uniform stress distribution. However, this increased thickness results in greater compliance of the joint, making it more susceptible to overall deformation under external loads. This trade-off between stress concentration and joint stiffness is critical for optimizing load transfer efficiency. Furthermore, failure modes shift with increasing adhesive thickness. For thinner adhesives (1.0 mm–2.0 mm), adhesive shear failure dominates, especially at the edges of the bond. For thicker adhesives (3.0 mm–4.0 mm), we observe a shift to more compliant failure modes, including adhesive debonding and potential adherend fracture. This suggests that thicker adhesives are less effective at transferring high tensile forces. This study presents a detailed analysis of **stress distributions** in **hybrid adhesive-bolt joints** and investigates the potential **failure modes** associated with these joints. The results show that **adhesive debonding** is the primary failure mechanism under typical **static tensile loads**, particularly in joints with **thin adhesive layers**. However, for joints with thicker adhesives or high preload in the bolt, **bolt yielding** and **aluminum plasticity** can become dominant failure modes. These findings provide valuable insight into optimizing joint design by considering the **adhesive thickness**, **bolt preload**, and material properties to prevent premature failure.

In practical terms, the adhesive layer provides critical stress dissipation under tensile loads. The results suggest that adhesive thickness should be optimized for the specific application based on the required stiffness and load-bearing capacity of the joint. For applications requiring high tensile strength and minimal deformation, thinner adhesives (1.0–2.0 mm) are preferred, while for applications requiring greater flexibility and shock absorption, thicker adhesives may be more suitable. Based on the findings of this study, the following recommendations are made for selecting adhesive thickness in hybrid bolt-adhesive joints:

For high-strength applications requiring minimal deformation, adhesive thicknesses in the range of 1.0–2.0 mm are optimal. These thicknesses provide a good balance between stress distribution and load transfer efficiency.

For applications requiring greater flexibility, such as shock absorption or fatigue resistance, adhesive thicknesses of 3.0–4.0 mm are more suitable, though they may reduce load-bearing capacity.

Aerospace applications, where both strength and stiffness are critical, should prioritize medium-thickness adhesives (1.0–2.0 mm), which optimize both stress dissipation and joint compliance.

In automotive applications, where dynamic loading and impact resistance are essential, thicker adhesives may be beneficial for damping vibrations but should be used with caution due to potential adhesive failure at high stresses.

4. Conclusions

This study highlights the significant impact of adhesive thickness on the performance of hybrid bolt-adhesive joints. Through finite element simulations of hybrid double-lap joints, the research reveals that adhesive thickness plays a crucial role in stress distribution, load transfer, and failure modes. The results indicate that medium-to-low adhesive thicknesses (1.0–2.0 mm) offer the best balance between reducing stress concentrations and optimizing load transfer efficiency for most static loading conditions. Conversely, thicker adhesives (3.0–4.0 mm) increase the joint's compliance but may compromise load efficiency and raise the risk of adhesive failure, particularly in joints requiring higher stiffness.

While the study provides valuable insights into the design of hybrid adhesive-bolt joints, several limitations remain. The analysis is based on numerical simulations and does not include experimental validation. Future research should focus on experimental studies to validate the findings, particularly under dynamic loading conditions, as the adhesive performance may vary under different operational environments. Furthermore, exploring the long-term durability of these joints under cyclic loading and environmental factors (e.g., temperature, humidity) will be essential to refine these recommendations for real-world applications.

In conclusion, the findings offer practical design guidelines for adhesive thickness based on joint stiffness, stress profiles, and load-bearing capacity. These insights are valuable for structural applications, including aerospace and automotive industries, where the balance between strength and flexibility is critical for joint performance.

References

Adams, R D. (2024). Prediction of the strength of adhesive lap joints. An investigative review. International Journal of Adhesion and Adhesives, 129, 103576. https://doi.org/10.1016/j.ijadhadh.2023.103576

Adams, Robert D. (2021). Adhesive bonding: science, technology and applications. Woodhead Publishing.

Adams, Robert D, Comyn, J., & Wake, W. C. (1997). Structural adhesive joints in engineering. Springer Science & Business Media.

Akkasali, N. K., Biswas, S., Sen, S., & Anitha, S. (2024). A state-of-the-art review on adhesively bonded joints of similar and dissimilar materials. Journal of Adhesion Science and Technology, 38(24), 4317–4371. https://doi.org/10.1080/01694243.2024.2384421

Alizadeh, M. H., Ajri, M., & Maleki, V. A. (2023). Mechanical properties prediction of ductile iron with spherical graphite using multi-scale finite element model. Physica Scripta, 98(12), 125270. https://DOI:10.1088/1402-4896/ad0d97

Aragon, A., Alegre, J. M., & Gutierrez-Solana, F. (2006). Effect of clamping force on the fatigue behaviour of punched plates subjected to axial loading. Engineering Failure Analysis, 13(2), 271–281. https://doi.org/10.1016/j.engfailanal.2005.01.010

Bektaş, İ. H., & Özer, H. (2024). Elastic and Viscoelastic Analysis of Stress Distribution in Single Lap Joints under Tensile Loading: Analytical and Numerical Approaches. Latin American Journal of Solids and Structures, 21(7), e556. https://doi.org/10.1590/1679-78258169

Campilho, R. D. S. G., Banea, M. D., Pinto, A. M. G., da Silva, L. F. M., & De httJesus, A. M. P. (2011). Strength prediction of single-and double-lap joints by standard and extended finite element modelling. International Journal of Adhesion and Adhesives, 31(5), 363–372. https://doi.org/10.1016/j.ijadhadh.2010.09.008

Chakherlou, T N, Shahriary, P., & Akbari, A. (2021). Experimental and numerical investigation on the fretting fatigue behavior of cold expanded Al-alloy 2024-T3 plates. Engineering Failure Analysis, 123, 105324. https://doi.org/10.1016/j.engfailanal.2021.105324

Chakherlou, Tajbakhsh Navid, & Abazadeh, B. (2011). Estimation of fatigue life for plates including pre-treated fastener holes using different multiaxial fatigue criteria. International Journal of Fatigue, 33(3), 343–353. https://doi.org/10.1016/j.ijfatigue.2010.09.006

Chan, W. S., & Vedhagiri, S. (2001). Analysis of composite bonded/bolted joints used in repairing. Journal of Composite Materials, 35(12), 1045–1061. https://doi.org/10.1177/002199801772662325

Choi, J.-I., Hasheminia, S. M., Chun, H.-J., Park, J.-C., & Chang, H. S. (2018). Failure load prediction of composite bolted joint with clamping force. Composite Structures, 189, 247–255. https://doi.org/10.1016/j.compstruct.2018.01.037

Esmaeili-Goldarag, F., Babaei, A., & Jafarzadeh, H. (2018). An experimental and numerical investigation of clamping force variation in

simple bolted and hybrid (bolted-bonded) double lap joints due to applied longitudinal loads. Engineering Failure Analysis, 91, 327–340. https://doi.org/10.1016/j.engfailanal.2018.04.047

Geiglou, Z. E., & Chakherlou, T. N. (2019). Numerical and experimental investigation of the effect of the cold expansion process on the fatigue behavior of hybrid (bonded bolted) double shear lap aluminum joints. International Journal of Fatigue, 126, 30–43. https://doi.org/10.1016/j.ijfatigue.2019.04.021

Goland, M., & Reissner, E. (1944). The stresses in cemented joints. https://doi.org/10.1115/1.4009336

Gopalan, R., & Narayanan, P. (2024). Experimental and numerical investigation of tensile-loaded staggered bolted and hybrid pultruded composite double lap joints. Journal of Adhesion Science and Technology, 38(11), 1895–1924. https://doi.org/10.1080/01694243.2023.2282825

Hart-Smith, J. (2021). Aerospace industry applications of adhesive bonding. In Adhesive bonding (pp. 763–800). Elsevier. https://doi.org/10.1016/B978-0-12-819954-1.00001-0

Karthikeyan, N., & Naveen, J. (2024). Progress in adhesive-bonded composite joints: A comprehensive review. Journal of Reinforced Plastics and Composites, 07316844241248236. https://doi.org/10.1177/07316844241248236

Kim, H. (2003). The influence of adhesive bondline thickness imperfections on stresses in composite joints. The Journal of Adhesion, 79(7), 621–642. https://doi.org/10.1080/00218460309578

Kushwah, S., Bhatt, M., Desai, C., Parekh, S., & Joshi, P. (2021). A methodological study for stress analysis to evaluate single lap adhesive joint. IOP Conference Series: Materials Science and Engineering, 1149(1), 012012. https://DOI: 10.1088/1757-899X/1149/1/012012

Li, M., Liu, Z., Yan, R., Lu, J., & Soares, C. G. (2022). Experimental and numerical investigation on composite single-lap single-bolt sandwich joints with different geometric parameters. Marine Structures, 85, 103259. https://doi.org/10.1016/j.marstruc.2022.103259

Lim, G.-H., Heidari-Rarani, M., Bodjona, K., Raju, K. P., Romanov, V., & Lessard, L. (2019). Mechanical characterization of a flexible epoxy adhesive for the design of hybrid bonded-bolted joints. Polymer Testing, 79, 106048. https://doi.org/10.1016/j.polymertesting.2019.106048

Maggiore, S., Banea, M. D., Stagnaro, P., & Luciano, G. (2021). A review of structural adhesive joints in hybrid joining processes. Polymers, 13(22), 3961. https://doi.org/10.3390/polym13223961

Malekzadeh, M., Shishesaz, M., Mosalmani, R., Maleki, V. A., & Yaghootian, A. (2025). Carbon Nanotube Reinforced 3D Printed PMMA Filaments: Mechanical Enhancement through Experimental and Multi-Scale Modeling. Materials Chemistry and Physics, 131194. https://doi.org/10.1016/j.matchemphys.2025.131194

Marchione, F. (2021). Analytical Stress Analysis in Single-Lap Adhesive Joints under Buckling Loads. International Journal of Engineering Transactions B, 34(02), 313–318.

Marchione, F. (2022). Effect of hollow adherends on stress peak reduction in single-lap adhesive joints: FE and analytical analysis. The Journal of Adhesion, 98(6), 656–676. https://doi.org/10.1080/00218464.2021.1995368

Marchione, F. (2025). Experimental and analytical investigation on the shear performance of double-lap adhesive joints with multi-layered adherends. Mechanics Research Communications, 145, 104400. https://doi.org/10.1016/j.mechrescom.2025.104400

Marchione, F., & Munafò, P. (2020). Experimental strength evaluation of glass/aluminum double-lap adhesive joints. Journal of Building Engineering, 30, 101284. https://doi.org/10.1016/j.jobe.2020.101284

Peres, L. M. C., Arnaud, M., Silva, A., Campilho, R., Machado, J. J. M., Marques, E. A. S., Dos Reis, M. Q., & Da Silva, L. F. M. (2022). Geometry and adhesive optimization of single-lap adhesive joints under impact. The Journal of Adhesion, 98(6), 677–703. https://doi.org/10.1080/00218464.2021.1994404

Pouraminian, M., Akbari Baghal, A. E., Andalibi, K., Khosravi, F., & Arab Maleki, V. (2024). Enhancing the pull-out behavior of ribbed steel bars in CNT-modified UHPFRC using recycled steel fibers from waste tires: a multiscale finite element study. Scientific Reports, 14(1), 19939. https://doi.org/10.1038/s41598-024-68682-3

Sekercioglu, T., & Kovan, V. (2008). Torque strength of bolted connections with locked anaerobic adhesive. Proceedings of the Institution of Mechanical Engineers, Part L: Journal of Materials: Design and Applications, 222(1), 83–90. https://doi.org/10.1243/14644207JMDA157

Disclaimer